Synthetic Nanoelectronic Probes for Biological Cells and Tissues

Bozhi Tian[1] and Charles M. Lieber[2]

[1]Department of Chemistry, James Franck Institute, and the Institute for Biophysical Dynamics, University of Chicago, Chicago, Illinois 60637; email: btian@uchicago.edu

[2]Department of Chemistry and Chemical Biology and School of Engineering and Applied Sciences, Harvard University, Cambridge, Massachusetts 02138; email: cml@cmliris.harvard.edu

Annu. Rev. Anal. Chem. 2013. 6:31–51

First published online as a Review in Advance on February 28, 2013

The *Annual Review of Analytical Chemistry* is online at anchem.annualreviews.org

This article's doi: 10.1146/annurev-anchem-062012-092623

Keywords

nanowire, field effect transistor, intracellular, extracellular, synthetic tissue

Abstract

Research at the interface between nanoscience and biology could yield breakthroughs in fundamental science and lead to revolutionary technologies. In this review, we focus on the interfaces between nanoelectronics and biology. First, we discuss nanoscale field effect transistors (nanoFETs) as probes to study cellular systems; specifically, we describe the development of nanoFETs that are comparable in size to biological nanostructures involved in communication through synthesized nanowires. Second, we review current progress in multiplexed extracellular sensing using planar nanoFET arrays. Third, we describe the designs and implementation of three distinct nanoFETs used to perform the first intracellular electrical recording from single cells. Fourth, we present recent progress in merging electronic and biological systems at the three-dimensional tissue level by use of macroporous nanoelectronic scaffolds. Finally, we discuss future developments in this research area, unique challenges and opportunities, and the tremendous impact these nanoFET-based technologies might have on biological and medical sciences.

1. INTRODUCTION

Semiconductor science and technology are a driving force in modern society due to the ever-increasing degree of miniaturization of semiconductor processing and transistor devices (1–6). To continue the remarkable success of semiconductor technology and perhaps produce new paradigms for logic, memory, and sensor devices, many researchers have been investigating devices based on synthesized nanostructures (2, 5, 7–12) in which geometries, organizations, and physical properties can be designed and controlled at the nanometer scale.

Many nanostructured materials have been designed and synthesized during the past several decades; these materials include colloidal nanoparticles (13, 14), semiconductor nanowires (NWs) (3, 4, 15, 16), and graphene (10, 17–20), in which properties distinct from their bulk counterparts have been discovered and exploited. For any class of nanostructured materials to become a platform for discovery and development, new structures and assemblies with tunable composition, morphology, and properties at different length scales must be obtained (3, 10, 18). Thus, semiconductor NWs are one of the most successful platforms currently available in nanoscience for several reasons. First, it is now possible to design NW structures de novo and to synthetically realize these structures with complex, yet controlled, modulations in composition (8, 16, 21–26), doping (16, 23), defect (27–29), and even topography (30–32). Second, this high degree of synthetic control enables the creation of NW building blocks that have predictable physical properties for testing fundamental limits of performance (5, 16). Third, it is possible to use these diverse NW building blocks to assemble hybrid or multicomponent functional materials in novel layouts and configurations (31, 33–45), allowing for rational exploration of the possible applications of multicomponent materials. Given these characteristics and capabilities, NWs are ideal for exploring what is possible in nanoscience and for creating new technologies. The nanoscience community has focused on these goals over the past decade and continues to do so because they overlap with those of other disciplines, such as synthetic biology (46–51).

Research at the interface between nanoscience and biology could yield breakthroughs in fundamental sciences and lead to revolutionary technologies (52, 53). Specifically, the exploration and application of semiconductor NW materials and devices in cellular systems could produce unprecedented interactions down to the molecular level. Such interactions have been utilized to gain knowledge relevant to human health by stimulating, recording from, and delivering objects to single cells and tissues in controlled ways to induce desired physiological responses, while minimizing undesirable effects (52, 53).

There are two types of NW-based platforms in biomedical sciences: basic platforms, which can be readily adapted to address biomedical questions, and advanced platforms, which are specifically designed to push the frontiers of what is possible by, for example, developing a new measurement tool. Basic platforms use conventional NW material and device systems with well-known physical or chemical properties, and they also have wide-ranging applications in many other fields, such as energy scavenging systems (54–61) and components for integrated circuits (34, 35). Basic platforms such as planar NW field effect transistors (FETs) (34, 35, 37, 40, 43) and vertical NW arrays (55–58, 60, 61) have been used in biomolecular sensing (52, 53), extracellular recording (52, 53), drug delivery (62–64), and localized cellular imaging (65). Advanced platforms have been designed to address intrinsic complexities in biology and medical sciences in a manner that had not previously been possible. Their target systems allow for new types or scales of interaction and measurements (31, 66–68) and thereby are providing new opportunities in science and technology. Examples of advanced platforms include recent intracellular FET probes (31, 67–69) and nanoelectronics-innervated synthetic tissues (66).

This review discusses the basic concept of nanoscale FETs (nanoFETs) and their applications in cellular electrophysiology. In Section 2, we describe the motivation behind nanoFET probes to study cellular systems versus existing recording technologies and the use of chemical synthesis to create nanoFETs de novo. In Section 3, we give an overview of progress in multiplexed extracellular sensing using planar nanoFET arrays. We describe electrical recordings at the single-cell, tissue, and organ levels and delineate their limitations and promises. In Section 4, we provide details about the main designs and implementation of nanoFETs in intracellular electrical recording from single cells, the first paradigm change in intracellular electrophysiology since the 1950s. We compare nanoFET-based techniques and conventional micropipette and microelectrode probes and describe the limits and future opportunities of these new probes. In Section 5, we introduce very recent progress in merging electronic and biological systems at the three-dimensional (3D) tissue level by introducing the new concept of macroporous nanoelectronic scaffolds (nanoES). We review the first-ever nanoelectronics-innervated synthetic tissues and discuss their applications. In the final section, we present our perspectives on future development in this research area, unique challenges and opportunities, and the tremendous impact that these nanoFET-based technologies might have on biological and medical sciences.

2. FUNDAMENTALS OF NanoFETs

2.1. Why and How are NanoFETs Applied in Biology and Medicine?

The ability to make electrical measurements inside single cells or throughout the entire 3D space of a tissue has many important implications for electrophysiology and biomedical sciences. The patch-clamp technique, in which a pulled-glass micropipette filled with electrolyte is inserted into a cell, offers intracellular electrical measurements with a high signal-to-noise ratio (S/N) and single-ion channel recording capability (70). The micropipette should be as small as possible to increase the spatial resolution and reduce the invasiveness of the measurement, and ideally should allow for recordings from subcellular structures. However, the overall performance of the technique also depends on the impedance of the interface between the micropipette and the cell interior (i.e., the smaller the probe tip size is, the larger the junction impedance), which sets limits on the temporal resolution and S/N of micropipette-based electrical probes (31, 41). Advanced techniques that involve the insertion of metal or carbon microelectrodes or nanoelectrodes into cells or tissues could be faced with a similar choice because all these tools are single-terminal devices and electrochemical thermodynamics, and kinetics must be considered for device operation (71–78). We discuss these techniques in detail below.

In integrated circuits, the basic device element is a multiterminal FET that uses either electrons or holes as the charge carriers (**Figure 1*a***) (79). Although the charge carriers are ions in biological systems, many biophysical links connect ions to electrons and holes in a FET. For example, the dynamic flow of ions in biological system can generate a spatially defined field potential (80). The Poisson equation (81) links such potentials directly to the ionic current sources and sinks that produce them. The Goldman–Hodgkin–Katz voltage equation (81) has also been used in cell membrane physiology to determine the equilibrium potential across a cell's membrane; it takes into account all of the ions that permeate through the membrane. The potentials, generated by ion flows and gradients, can function as gate signals to modulate the electrical output in FET devices (**Figure 1*b*,*c***). The sensitivity of a FET, or how well the transistor can receive and amplify the gate signal, is usually defined as transconductance (6, 52, 53, 79), which is inversely proportional to the dimension of the active device (6). Thus, nanoelectronics should have better sensitivity than

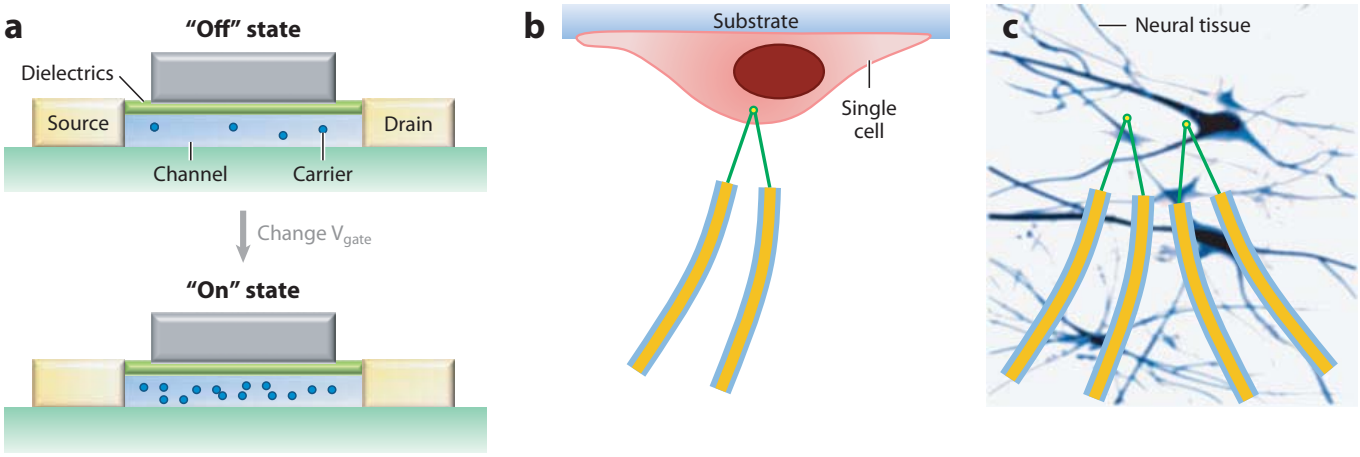

Figure 1

Field effect transistor (FET) basics and electrical interfaces between nanoscale FETs (nanoFETs) and biological systems. (*a*) A planar FET. Current flows along a semiconductor path known as the channel. At one end of the channel is an electrode termed the source. At the other end of the channel is an electrode termed the drain. The third electrode, which applies a voltage to the channel, is termed the gate, which modulates the electron/hole carrier density and the output of the FET. A small voltage change in the gate signal can cause a large variation in the current from the source to the drain, which is how the FET works and, in particular, amplifies signals. (*b*,*c*) Electrically based cellular sensing performed with a kinked nanoFET, in which (*b*) intracellular potentials (*c*) or extracellular field potentials can be used to change the nanoFET conductance. This change is analogous to applying voltage with a gate electrode.

its bulk and planar counterparts. As discussed in the following sections, nanoFETs can record electric potentials inside cells (31, 67–69) and from the internal regions of synthetic tissues (66), and because their performance does not depend on impedance, they can be made much smaller than micropipettes and microelectrodes. Moreover, nanoFET arrays are better suited for multiplexed measurements (67, 68).

2.2. Chemical Synthesis of NanoFETs

Three distinct classes of de novo design and synthesis have been used to yield nanoFET building blocks; they cover structural motifs in one, two, and three dimensions (**Figure 2**). The basic semiconductor NW (**Figure 2*a***) has a uniform composition; it is a one-dimensional (1D) structure with a diameter typically in the range between 3 and 500 nm. In the growth process, which builds upon earlier research showing vapor–liquid–solid (VLS) growth of micrometer- to millimeter-diameter wires (82, 83), the nanocluster catalyst (typically gold nanoparticles) forms a liquid solution with NW reactant component(s) and, when supersaturated, acts as the nucleation site for crystallization and preferential 1D growth (84, 85). Other growth mechanisms, such as vapor–solid–solid (VSS) and vapor–solid (15), can also be explored to yield high-quality semiconductor NWs. Within this framework, it is straightforward to synthesize NWs with different compositions, such as group III–V, IV, and II–VI semiconductors (8, 15, 86, 87), using the appropriate nanocluster catalysts and growth temperatures/pressures. Additionally, NW structures in which the composition, dopant, and even growth mechanisms (e.g., VLS, VSS) are modulated along axial (**Figure 2*b***) (21, 22, 88–90) or radial (25, 29, 91) directions have also been widely exploited. These axial and radial NW heterostructures have many advantages, compared with homogeneous semiconductor NWs, and they have proven exceptionally powerful for a broad range of electronic, photonic, and optoelectronic device applications (16). For example, germanium–silicon core-shell NWs have been chemically synthesized for high-mobility NW FETs due to

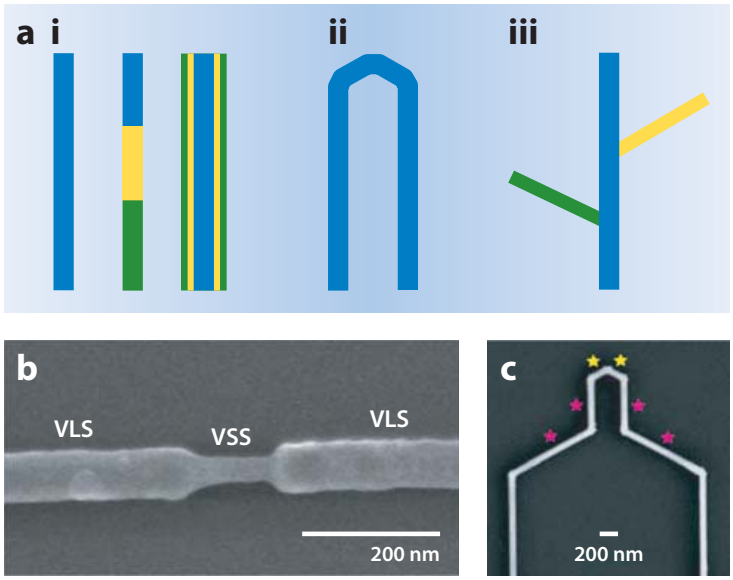

Figure 2

Semiconductor nanowire structural motifs for nanoscale field effect transistors. (*a*) One-dimensional (1D), two-dimensional (2D), and three-dimensional (3D) motifs. (*i*) A 1D motif may have uniform composition and doping (*left*) or may be axially (*middle*) or radially (*right*) modulated. (*ii*) A nanowire with structurally coherent kinks, introduced in a controlled manner during axial elongation, represents an example of a 2D motif. (*iii*) Heterobranched nanowires yield a 3D structure, and the branch junction (e.g., the junction between the blue and yellow segments) can be exploited for localized sensing. (*b*) An axial nanowire heterostructure made by modulation in vapor–liquid–solid (VLS) and vapor–solid–solid (VSS) growth mechanisms. (*c*) A multiply kinked nanowire showing a probe structure. The yellow and magenta stars denote *cis* and *trans* conformations, respectively. Modified from References 31 and 88 with permission from the American Association for the Advancement of Science and the American Chemical Society.

quantum confinement of carriers within the germanium core by the larger-bandgap silicon shell (5, 92–95).

We recently demonstrated the second structural motif by an approach in which topological centers are synthetically introduced in a controlled manner in linear 1D structures (**Figure 2*a***) (31, 32). In this study, we showed that iterative control over nucleation and growth leads to kinked NWs, in which the straight sections are separated by triangular joints; doping can be varied at these topologically defined points (**Figure 2*c***). Moreover, akin to organic chemistry, new research shows that it is possible to control the stereochemistry of adjacent kinks to allow the synthesis of increasingly complex two-dimensional (2D) and 3D structures; this research represents a great opportunity for the future in terms of synthesis of nanostructures with arbitrary geometries and properties. (31).

The third basic motif involves the synthesis of branched or tree-like NW structures (**Figure 2*a***) (24, 26, 96). To this end, we reported a rational, multistep approach toward the general synthesis of 3D branched NW heterostructures (24). Single-crystalline semiconductors, including those in groups IV, III–V, and II–VI, and metal branches were selectively grown on core or core-shell NW backbones, and the composition, morphology, and doping of core or core-shell NWs and branch NW swell were controlled during synthesis. Although the first structural motif has been the most extensively used as building blocks of basic platforms, the second and third motifs are much more structurally and functionally complex, and they have great potential in bottom-up synthesis to yield increasingly powerful functional components of advanced platforms.

3. MULTIPLEXED EXTRACELLULAR ELECTRICAL RECORDING

3.1. Why Use NanoFETs for Multiplexed Extracellular Recording?

Natural and synthetic cellular assemblies are usually organized into 2D or 3D hierarchical networks operating on spatial and temporal scales that span many orders of magnitude. Advances in microfabrication of high-density passive multielectrode arrays (MEAs) and active transistor arrays on silicon substrates permit direct electrical recording down to ~10-μm length scales; importantly, however, signals recorded within ~100 μm are often correlated (4–6), and it is difficult to resolve cellular signals at the single-cell level. As discussed above, simply reducing the size of individual metal electrodes to achieve more localized detection is not viable because of corresponding increases in their impedance (7, 8), which intrinsically limits the resolution of such passive recording devices.

Several characteristics of silicon NW nanoFET arrays make them unique for high-resolution multiplexed extracellular recording from cellular systems. First, as previous studies have shown, NW nanoFETs can achieve ultrahigh-sensitivity detection of charged biomolecules, including single particles (53). Second, bottom-up fabrication of nanoFETs yields devices that have nanoscale protrusions from the substrate surface (53, 97). These protrusions can reduce device-to-cell/tissue separation and promote enhanced cell–nanostructure interaction. They have also yielded high-S/N extracellular recordings of field potentials from cultured cells and cardiac tissue whose signals are better than those of planar FETs. Third, the bottom-up approach enables high-performance nanoFET fabrication on transparent, flexible, and stretchable substrates (34, 38–40). The ability to design device structures and arrays on substrates that are adapted to specific biological applications also introduces new possibilities for interfacing with living tissues, such as bioresorbable and implantable devices (98–101). This capability also allows one to perform other measurements or manipulations, such as high-resolution optical imaging, in conjunction with nanoFET recordings. Fourth, the active junction area of typical nanoFETs, which measures 0.01–0.1 μm^2, is much smaller than those of MEAs and planar FETs, which are 10^2 to 10^5 times larger, and can provide better spatial resolution of the signals (41). Finally, nanoFET detectors provide a fast intrinsic response time, which is critical for high–temporal resolution recordings (95, 102).

3.2. Electrical Interfacing with Cultured Neurons

An early example of a multiplexed nanoFET recording layout consisted of a neonatal rat cortical neuron and four peripheral silicon nanoFETs that were arranged at the corners of a rectangle, in which polylysine patterning was used to promote axon and dendrite growth across single nanoFETs (**Figure 3*a***) (103). This multiplexed nanoFET/neurite hybrid was used to study spike propagation; one NW was used as a local input to elicit action potential spikes. Following stimulation with a biphasic pulse sequence, back propagation of the elicited action potential was detected in the two dendrites crossing the second and third NWs. The lack of observed signal from the fourth NW demonstrated the absence of cross talk in the hybrid device array and, thus, the device's capacity for multiplexed subcellular resolution detection.

3.3. Recording from Cardiomyocyte Monolayers

Our group also carried out multiplexed measurements by using nanoFET arrays interfaced with cultured embryonic chicken cardiomyocytes (**Figure 3*b***) (33). The nanoFETs were patterned in a linear array with an average spacing of 300 μm to characterize the signal propagation within

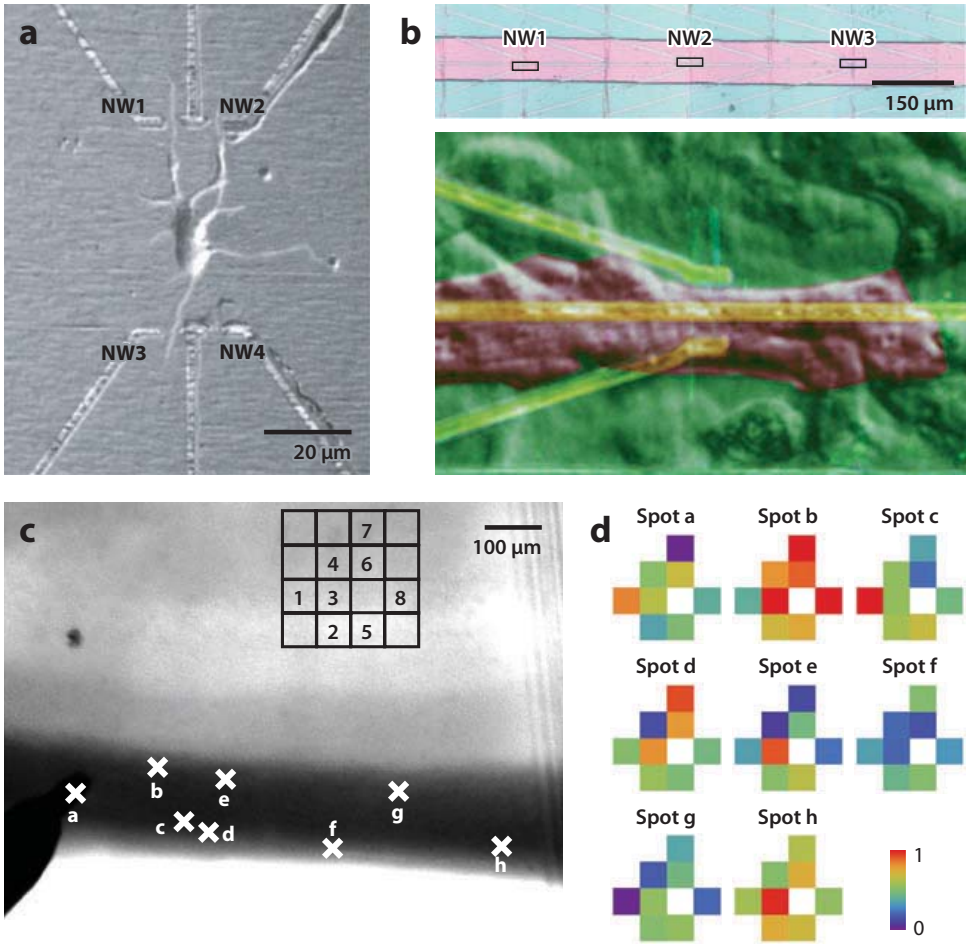

Figure 3

Multiplexed extracellular electrical recordings obtained with nanoscale field effect transistors (nanoFETs). (*a*) Optical image of a cortical neuron interfaced to three of the four functional nanoFETs in an array. (*b*) (*Top*) Optical micrograph of three nanoFET devices [nanowire (NW)1, NW2, and NW3] in a linear array. The area with exposed NW devices is shown in pink. (*Bottom*) A false-colored differential interference contrast bright-field image of individual cardiomyocytes (*purple*) and single nanoFETs (*yellow*). (*c*) Optical image of an acute slice over a four-by-four NW FET array. Signals were recorded simultaneously from the eight devices shown. Crosses along the lateral olfactory tract fiber region of the slice correspond to stimulation spots *a–h*. The stimulator insertion depth was not precisely controlled in these experiments. (*d*) Maps of the relative signal intensity or activity for the eight devices. Modified from References 33, 41, and 103 with permission from the American Association for the Advancement of Science.

cardiomyocyte monolayers. Recordings from multiple nanoFETs that were in contact with spontaneously beating monolayers yielded very stable and high-S/N (>10) field potential spikes. In this experiment, the relatively large signal magnitude confirmed that a good junction was formed between each nanoFET and the polydimethylsiloxane/cell substrate. Additionally, we used a cross-correlation method to robustly determine the time differences between the signals recorded by the devices. The time shifts between devices and device separations yielded propagation speeds between 0.07 and 0.21 m s^{-1}, which are consistent with other measurements on cardiomyocyte monolayers. The variation in propagation speeds in this study is not surprising, given the monolayer inhomogeneity, and suggests an important future direction. We propose that high-resolution multiplexed nanoFET recordings, together with optical imaging, will enable intercellular propagation to be characterized in detail for well-defined cellular structures.

3.4. Recording from Tissues and Organs

Finally, nanoFETs have been used to probe electrical activity in tissues and organs (41, 42). To this end, we studied the activity patterns of layer II/III cells in the piriform cortex of acute rat brain slices by stimulating different sets of axon fibers in the lateral olfactory tract (LOT). In a representative experiment, we simultaneously monitored eight devices within a four-by-four 2D array, oriented under the pyramidal cell layer of an acute slice, following stimulation at eight different spots in the LOT (**Figure 3*c***) (41). Strong stimulation of all axon fibers in the LOT yielded similar responses from the eight nanoFETs; the population spike signals (postsynaptic activities) were clear regardless of the stimulation position. Reduced stimulation intensity was also employed so that at each spot only a subgroup of fibers was activated. Notably, visual inspection of 2D activity maps for each of the eight stimulation positions revealed how heterogeneous activity can be resolved (**Figure 3*d***) and, thus, identified complex functional connectivity in the piriform cortex.

3.5. Challenges and Promises

Although great progress has been made in extracellular electrical recordings obtained with NW nanoFETs, many challenges remain. For example, there remains a pressing need to further enhance the nanoFET S/N so that very weak endogenous biological signals, with an amplitude of ~100 μV, can be readily resolved. We could achieve this goal through (*a*) a new chemical design and synthesis of high-mobility NW building blocks for nanoFETs or (*b*) nanoscale engineering of NW materials to reduce nanoFET noise by, for example, thermal annealing and/or surface passivation.

Importantly, the high-input impedance of nanoFETs circumvents the common challenges posed by implanted microelectrodes, in which gradual increases of single-terminal device impedance arising from, for example, absorption of proteins decreases the S/N over time (41, 104, 105). This property makes nanoFETs very promising for multiplexed, in vivo chronic recordings, especially because (*a*) the nanoscale device size allows one to integrate multiple nanoFETs into minimally invasive and movable electrophysiological probes (68), (*b*) bottom-up fabrication permits one to choose biocompatible or even biodegradable materials as substrates to reduce mechanical mismatch and to minimize inflammatory tissue response (31, 66, 68, 98–101), and (*c*) the nanoscale topology could be arbitrarily designed de novo to promote better attachment of single cells or even intracellular contacts. Therefore, nanoFETs should lead to many exciting opportunities to interface living tissues and organs with electronics for biomedical applications (e.g., diagnostic devices for brain trauma treatment and surgical tools for cardiac therapy), and even new cybernetic biosystems for hybrid information processing.

4. INTRACELLULAR ELECTRICAL RECORDING

4.1. Why Intracellular?

As the key component of cells, lipid membranes play important structural and protective roles and form a stable, self-healing, and virtually impenetrable barrier to ions and small molecules (106). Because these membranes have resistance and capacitance, the membrane resistance–capacitance circuit also behaves as an electrical barrier, and it attenuates and even distorts intracellular signals as they are detected by extracellular sensors. More importantly, although cellular signal transduction often begins when extracellular signaling molecules activate a cell-surface receptor, it is the subsequent intracellular processing that eventually causes a cellular response. Deciphering such intracellular signal transmission and amplification

processes is critical to our understanding of cellular information flow and cell physiology. Therefore, it is highly desirable to deliver nanoFETs into a cell and to directly record intracellular electrical activities, which can provide much more detailed information about how cells work.

4.2. Why Use NanoFETs for Intracellular Recording?

Although nanoFETs have been exploited for ultrasensitive detection of biological markers and high-resolution extracellular recording from cells (53), localized and tunable intracellular sensing and recording had not been demonstrated prior to our studies, because all FETs and nanoFETs were created on planar substrates by use of the basic nanoFET platform. Ideally, rather than force the cell to conform to the substrate, a movable and 3D nanoFET with the necessary source and drain electrical connections should make contact with the cell and probe the cell membrane. However, before 2010, minimally invasive insertion of a nanoFET into the confined 3D space of a single cell, or even into 3D cellular networks, still posed a major challenge because the source and drain typically dominated the overall device size and defined a planar and rigid structure, regardless of whether the nanoFET was on or suspended above a substrate. An advanced nanoFET platform that is designed specifically for intracellular measurement is needed to meet this requirement (32, 67–69). **Figure 4*a*** depicts three distinct examples that we have recently introduced to address this central challenge; they include a kinked NW nanoFET, a branched intracellular nanotube nanoFET, and active nanotube nanoFET devices.

Existing probes that are capable of intracellular sensing and recording include voltage-sensitive optical dyes and proteins (107–110) and single-terminal glass or carbon microelectrodes (**Figure 5**) (70, 72). Voltage-sensitive dyes can readily be used to interrogate action potentials with high spatial resolution, but they are limited in terms of S/N, pharmacological side effects, phototoxicity, and difficulty in differentiating single spikes (108). For electrical probes (**Figure 5**), the single electrical connection allows for mechanical insertion into cells, but the requirement of direct ionic and/or electrical junctions between the probe tip and the cytosol introduces several limitations. First, the tip size of such probes (~0.2 to 5 μm) is a compromise between being small enough (<5 μm) to penetrate or rupture the cell membrane with minimal damage and large enough (>0.2 μm) to yield a junction impedance that is sufficiently low for small cellular signals to be discerned from thermal noise. Second, direct exposure of intracellular species to extraneous probe surfaces or electrolytes in probe lumen, especially for large glass micropipettes, might induce irreversible changes to cells and thereby prevent long-term and noninvasive cellular recording. Finally, these probe techniques are intrinsically passive and incapable of built-in signal processing and facile integration with other circuitries. This limitation is especially important given the increasing need for cell–machine communication (111–114).

NanoFETs can function in the sub–10-nm regime (2). In principle, their exceptionally small size enables them to function as mechanically noninvasive probes that can enter cells through endocytic pathways, as can occur with nanoparticles (115–118). Moreover, when interfacing with cells, nanoFETs process input and output information without the need for direct exchange with cellular ions; thus, interfacial impedance and biochemical invasiveness can be ignored or minimized (**Figure 5**). Also, because signals are transduced by changes in field or potential at well-isolated surfaces, nanoFETs can detect cellular potential, as well as biological macromolecules, and could be employed for multiplexed intracellular measurements. Until recently, investigators could not take advantage of these properties; however, our recent studies (**Figure 4*a***) (31, 67–69) have revealed three solutions to this problem.

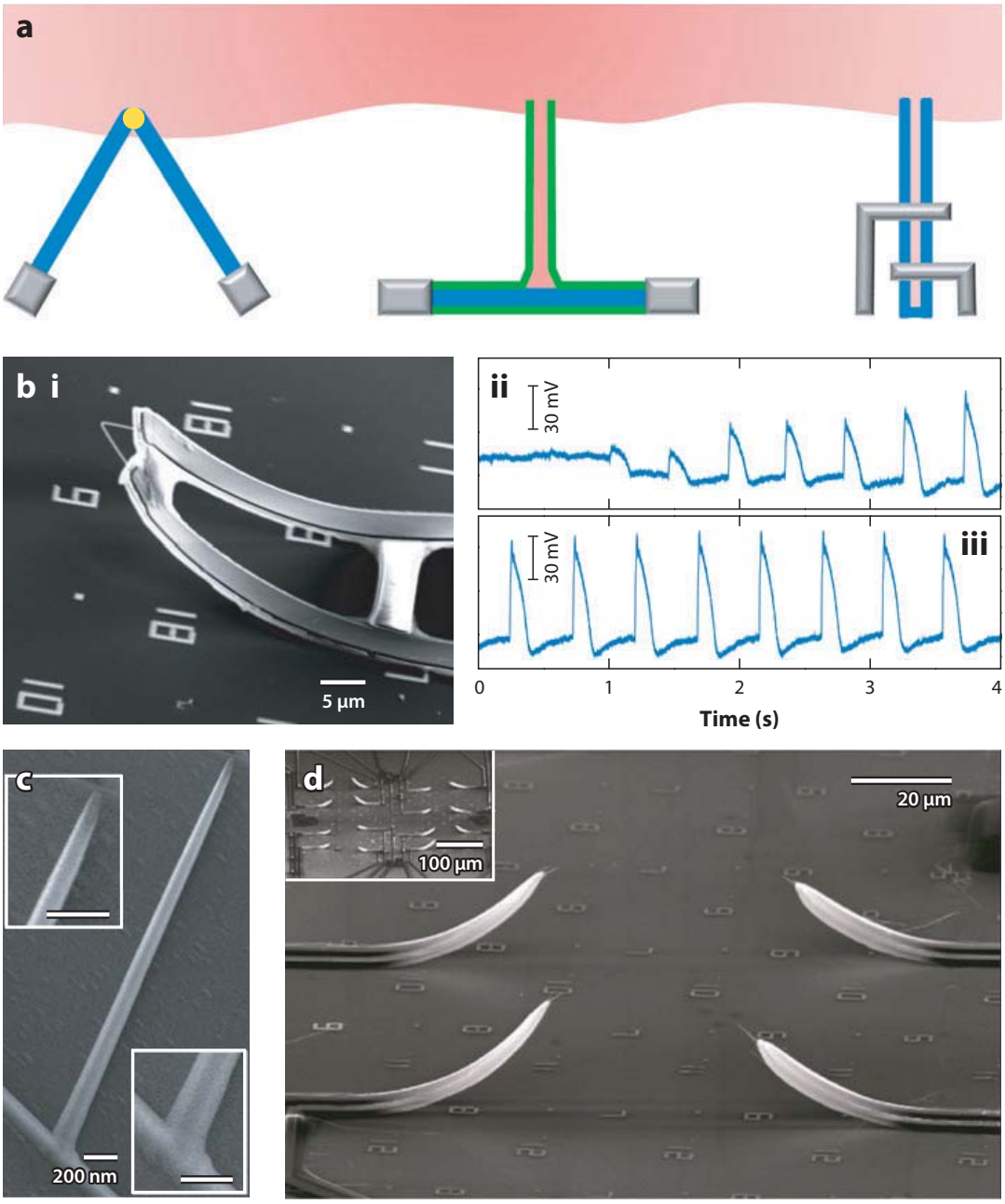

Figure 4

Intracellular electrical recordings using nanoscale field effect transistors (nanoFETs). (*a*) (*Left*) A kinked nanowire nanoFET. (*Middle*) A branched SiO_2 nanotube synthetically integrated on top of a nanoFET (BIT-FET probe). (*Right*) An active nanotube transistor (ANTT) probe. (*b*) (*i*) Scanning electron microscope (SEM) image of a kinked nanoFET probe. (*ii*, *iii*) Its intracellular electrical recordings from spontaneously beating cardiomyocytes. (*c*) SEM image of a BIT-FET probe. (*Insets*) The tip and root parts of the hollow branch. Scale bars, 200 nm. (*d*) SEM image of an ANTT probe array. Modified from References 31, 67, and 68 with permission from the American Association for the Advancement of Science, Nature Publishing Group, and the American Chemical Society.

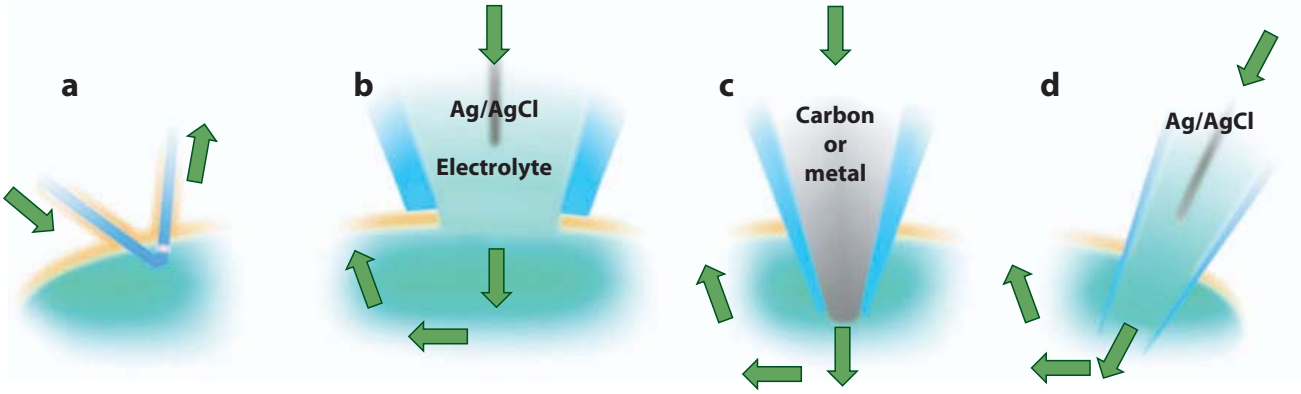

IC technique	Equivalent circuit	Size (nm)	Calibrations	Capabilities	Invasiveness	Cellular entrance
Glass micropipette (b, d)	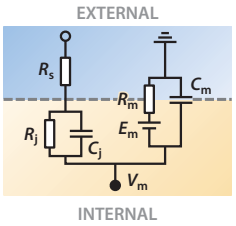	~50–5,000 Impedance limited	Both amplitude and shape	Can record both current and voltage Single ion channel to whole-cell recording	Electrochemical and mechanical	Mechanical or electrical
Carbon or metal micro-/ nanoelectrode (c)		~500–1,000 Impedance limited	Both amplitude and shape	Can record both current and voltage Whole-cell recording	Electrochemical and mechanical	Mechanical or electrical
NanoFET (a)	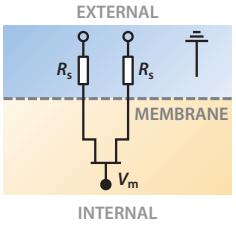	~10–100	Amplitude	Can record only voltage Whole-cell recording Multiplexing is scalable High spatiotemporal resolution	Minimal	Biological

Figure 5

(*a*) A comparison between a kinked nanoscale field effect transistor (nanoFET) probe and (*b–d*) conventional intracellular tools. The green arrows indicate the current flows. Abbreviations: C_j, junction capacitance; C_m, membrane capacitance; IC, intracellular electrical recording; R_s, series resistance; R_j, junction resistance; R_m, membrane resistance; V_m, intracellular potential.

4.3. Designs and Implementation of Intracellular NanoFET Probes

In 2010, the first nanoFET intracellular probes were designed and chemically synthesized without lithography to encode an ~100-nm FET device at the apex of a kinked NW (**Figure 4*a*,*b***) (31). These probes were created through control over *cis* and *trans* conformations and modulation doping during the silicon NW synthesis (31, 32). Subsequently, the free arms of these kinked NWs were electrically contacted to freestanding, flexible electrodes. Electrical characterization of the 3D NW probes showed that they were robust to mechanical deformation, recorded solution pH changes with high resolution, and when modified with phospholipid bilayers, recorded the intracellular potential of single cells. Significantly, electrical recordings of spontaneously beating cardiomyocytes demonstrated that, for the first time, 3D nanoFET probes continuously monitored extra- to intracellular signals during cellular uptake. The nanometer size of these active semiconductor nanoprobes, their biomimetic surface coating, and their flexible 3D geometry make them a powerful tool for intracellular electrophysiology.

Kinked nanoFET–based intracellular recordings represent the first example of the intracellular combination of semiconductor devices and cells, but the kink configuration and device design place certain limits on the probe size and the potential for multiplexing. To address these issues, we created a new device platform in which a branched SiO_2 nanotube was synthetically integrated on top of a nanoFET (BIT-FET) (**Figure 4*a*,*c***) (67). This branched nanotube penetrated the cell membrane to bring the cell cytosol into contact with the extracellular FET, thereby enabling intracellular recording of transmembrane potential. Studies of cardiomyocytes demonstrated that when phospholipid-modified BIT-FETs are brought close to cells, the nanotubes spontaneously penetrate the cell membrane and yield full-amplitude intracellular action potentials; a stable, tight seal forms between the nanotube and the cell membrane. Significantly, we also showed that multiple BIT-FETs can be used for multiplexed intracellular electrical recordings from both single cells and networks of cells.

Recently, we also demonstrated a conceptually new and practically simple nanoFET probe that consists of a single semiconductor nanotube (**Figure 4*a*,*d***) (68). Fabrication of the active nanotube transistor (ANTT) intracellular probe involves attaching source/drain contacts to one end of a silicon or other semiconductor nanotube and electrically isolating these source/drain contacts from the surrounding medium. Then, the solution filling the interior of the nanotube "gates" the transistor, and the variation of the interior electrochemical potential is recorded as a change in device conductance. In our experiments, the free ends of the ANTT probes were inserted into cardiomyocytes, and the time-dependent changes associated with action potential spikes were recorded by this nanoFET probe. As expected, when a similarly configured solid NW nanoFET was inserted into the cell, no signal was observed because it was not possible to gate the nanoFET. Finally, we prepared multiple ANTTs at the ends of single probes, which enabled multiplexed recording of full-amplitude intracellular action potentials from single cells and multiplexed arrays of single–ANTT device probes (**Figure 4*d***).

4.4. Challenges and Promises

Despite these developments, more research is needed to advance nanoFET-based intracellular measurement techniques (**Figure 5**). For example, the S/N of nanoFETs is no better than that of glass micropipette recordings, although the spatial resolution of the former is much higher. Current nanoFET designs allow only potential recordings, but measurements of ionic currents could be performed if other signal transduction mechanisms are combined with nanoFETs. Moreover, nanoFETs are not yet capable of cell stimulation, in addition to recording. Nevertheless, we believe that the advantages of nanoFET intracellular probes used in our studies—including their sub-10-nm sizes; ease of operation (e.g., no need to compensate or calibrate the probe junction potential and capacitance); lipid fusion–assisted cellular entrance**;** minimal mechanical and biochemical invasiveness; and potential for large-scale, high-density, multiplexed recordings—make them very attractive new measurement tools that will substantially broaden the scope of fundamental and applied electrophysiology studies to regimes that are difficult to access by current methods. For example, an exciting future application of these nanoFET probes will be measuring membrane potentials directly from cellular organelles, a holy grail in intracellular electrophysiology.

5. NANOELECTRONICS INNERVATED SYNTHETIC TISSUES

The development of synthetic 3D macroporous biomaterials as extracellular matrices (ECMs) is crucial because (*a*) functionalized 3D biomaterials allow for studies of cell and tissue development in the presence of spatiotemporal biochemical stimulants (119, 120) and (*b*) the understanding

of pharmacological response of cells in 3D (121–123) can provide a more robust link to in vivo disease treatment compared with that from 2D cell cultures. Further development of biomaterials requires the capability to monitor cells throughout the 3D microenvironment.

Recent efforts to couple electronics and tissues have focused on flexible, stretchable planar arrays that conform to tissue surfaces (10, 42, 53, 98–101) or implantable microfabricated probes (124). These approaches have been used to probe electrical activities near the surface of the heart, brain, and skin, and they have translational potential. However, these new electronic tools have a limited ability to merge electronics with tissues throughout 3D space while minimizing tissue disruption both because of the 2D support structures and because the electronic sensors are generally much larger than the ECM and cells. Our studies using nanoFETs have shown that electronic devices with nanoscopic features can detect extra- and intracellular potentials from single cells, but they were also limited to surface or near-surface recordings from tissue and organs (42, 53). The seamless integration of electronics throughout tissues (**Figure 6*a***) remained a major challenge. To address this challenge, we recently proposed certain constraints (66): (*a*) The electronic structures must be macroporous, not planar, to enable 3D interpenetration with biomaterials; (*b*) similar to biomaterial scaffolds, the electronic network should be on the nanometer or micrometer scale; and (*c*) the electronic network must have 3D interconnectivity and mechanical properties similar to those of biomaterials (**Figure 6*b***).

5.1. A New Concept of Merging Electronics with Cellular Systems

We have integrated nanoelectronics into tissues in three dimensions, and this integrative synthetic approach involved stepwise incorporation of biomimetic and biological elements into nanoelectronic networks across nanometer to centimeter scales (**Figure 6*a***) (66). First, chemically synthesized kinked or uniform silicon NWs were registered and electrically connected to yield FETs (**Figure 6*a***), forming the nanoelectronic sensor elements for hybrid biomaterials. Second, individual nanoFET devices were arranged and integrated into freestanding macroporous scaffolds (**Figure 6*a***), termed nanoES. The nanoES were tailored to be 3D, to have nanometer to micrometer sizes and high (>99%) porosity, and to be highly flexible and biocompatible. The nanoES could also be hybridized with biodegradable synthetic ECMs to create suitable cellular microenvironments prior to tissue culture. Finally, cells were cultured inside nanoES or hybrid nanoES (**Figure 6*a***); subsequently, biological species were generated and the cells were merged with the nanoelectronics in three dimensions. The entire biomimetic process made a natural transition from an electronic system to a biological one through integration of the third component, nanoES, into the synthetic tissues (**Figure 6*c***). We did not use metal electrodes or carbon nanotube/nanofiber–based passive detectors because impedance limitations (i.e., S/N and temporal resolution that degrade as the area of the metal or carbon electrodes is decreased) make it difficult to reduce the size of individual electrodes below that of a cell, a size regime necessary to achieve noninvasive 3D interface of electronics with cells in tissue.

5.2. Designs and Preparation of Synthetic Tissues

We have designed two types of 3D macroporous nanoES (reticular and mesh nanoES) to mimic the structure of natural tissue scaffolds (**Figure 7**) (66). These nanoES were formed through self-organization of coplanar reticular networks with built-in strain (**Figure 7*a***) and through manual manipulation of 2D mesh matrices (**Figure 7*b***). The scaffolds exhibited robust electronic properties and could be either used alone or seamlessly merged with other biomaterials to form biocompatible extracellular scaffolds for efficient 3D cultures of neurons, cardiomyocytes, and smooth muscle cells (**Figure 7*c*,*d***). Furthermore, we obtained multiplexed electrical recordings

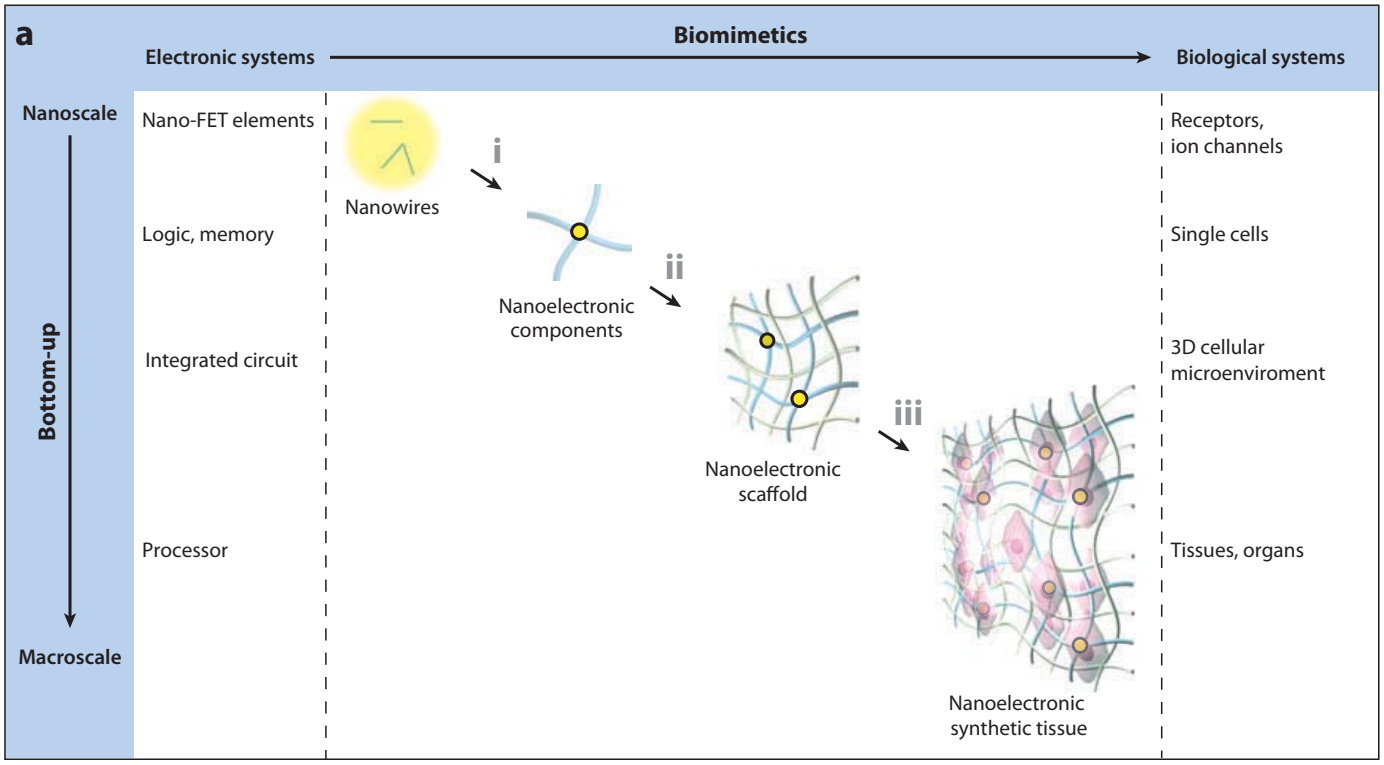

b

	Targets	Approaches	Implementation examples	Steps		
Biomimetics	Composition	+ Synthetic polymer	Deposit PLGA, alginate	i	ii	
		+ Natural polymer	Add or secrete collagen, polysaccharides		ii	iii
		+ Cellular species	Biosynthesize proteins and lipids			iii
		– Electronic materials	Reduce silicon, metals, dielectrics	i	ii	
	Structure	+ Porosity	Increase to >90%	i	ii	
		– Feature size	Decrease to submicrometer	i	ii	
	Mechanics	+ Flexibility	Decrease bending stiffness to <10 nN m	i	ii	iii
		+ Stretchability	Use serpentine device designs	i	ii	iii
	Biofunctions	+ Morphogenesis	Enable cell growth and proliferation			iii
		+ Other signals	Activate ECM cues		ii	iii
		– Cytotoxicities	Use biocompatible materials	i	ii	

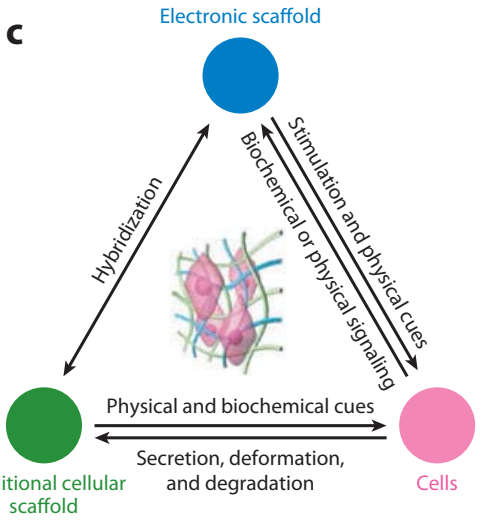

Figure 6

Integration of nanoelectronics with cells and tissues. Conventional bulk electronics are distinct from biological systems in terms of composition, structural hierarchy, mechanics, and function. Their electrical coupling at the tissue or organ level is usually limited to the tissue surface, where only boundary or global information can be gained unless invasive approaches are used. (*a*) In a new concept, an integrated system can be created from discrete electronic and biological building blocks (for example, semiconductor nanowires, molecular precursors of polymers, and single cells). There are three biomimetic and bottom-up steps: (*i*) patterning, metallization, and epoxy passivation of single-nanowire field effect transistors (FETs); (*ii*) formation of three-dimensional nanowire FET matrices (nanoelectronic scaffolds) by self- or manual organization and hybridization with traditional extracellular matrices (ECMs); and (*iii*) incorporation of cells and growth of synthetic tissue through biological processes. Yellow dots, nanowire components; blue ribbons, metal and epoxy interconnects; green ribbons, traditional ECMs; pink shading, cells. (*b*) Rationale and approaches for the biomimetic implementation of nanoelectronics-innervated synthetic tissues. The steps correspond to those used in panel *a*. (*c*) The new electronic scaffold component in synthetic tissues enables additional interactions with the traditional cellular scaffold and cells. Abbreviation: PLGA, poly(lactic-*co*-glycolic acid).

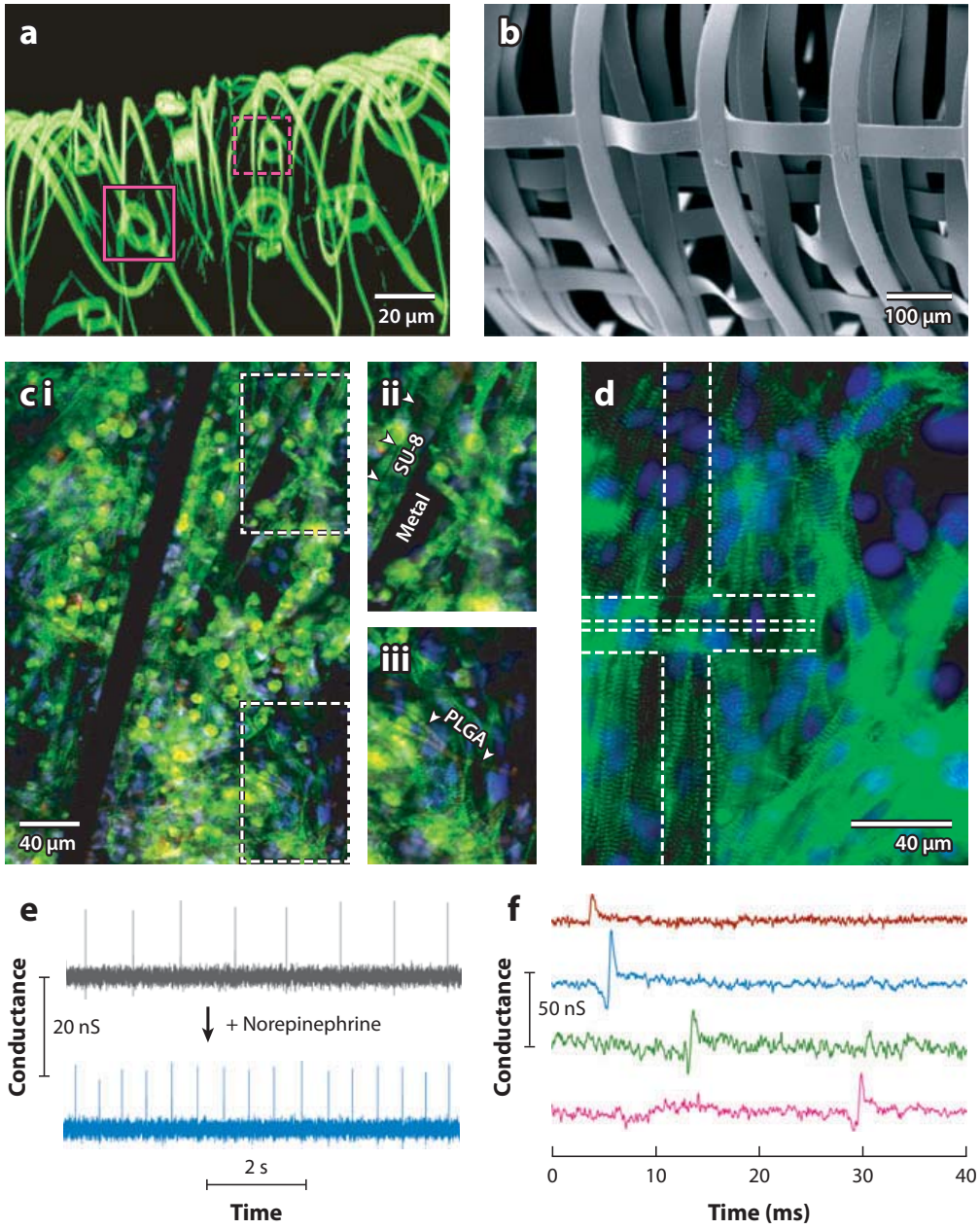

Figure 7

Nanoelectronic scaffolds (nanoES) and synthetic tissues. (*a*) Three-dimensional reconstructed confocal fluorescence micrographs of reticular nanoES. The scaffold was labeled with rhodamine 6G. Solid and dashed magenta squares indicate two nanowire field effect transistors (FETs) located on different planes. (*b*) Scanning electron microscope image of a loosely packed mesh nanoES, showing its macroporous structure. (*c*) (*i*) Confocal fluorescence micrograph of a synthetic cardiac patch. (*ii*,*iii*) Zoomed-in views of the upper and lower dashed regions in part *i*, showing metal interconnects, the SU-8 scaffold (arrowheads in part *ii*) and electrospun poly(lactic-*co*-glycolic acid) (PLGA) fibers (arrowheads in part *iii*). (*d*) Epifluorescence micrograph of the surface of the cardiac patch. Green (Alexa Fluor 488), α-actin; blue (Hoechst 34580), cell nuclei. The position of the source–drain electrodes is represented by dashed lines. (*e*) Conductance-versus-time traces recorded from a single-nanowire FET before (*black*) and after (*blue*) the application of norepinephrine. (*f*) Multiplex electrical recording of extracellular field potentials from four nanowire FETs in a mesh nanoES. Data are conductance-versus-time traces of a single spike recorded at each nanowire FET. Modified from Reference 66 with permission from Nature Publishing Group.

of extracellular field potentials from 3D nanoelectronic innervated cardiac patches; for example, the sensors recorded the effects of drugs (**Figure 7*e*,*f***). These results suggest that it is feasible to perform continuous electrical monitoring of engineered tissue in three dimensions for in vitro therapeutic assays. Finally, we used 3D distributed nanoelectronic devices for simultaneous monitoring of pH both inside and outside an engineered tubular vascular construct that was developed from the nanoES; this study indicates that there is potential for multifunctional prosthetics.

5.3. Challenges and Promises

These results have led to a new field of research, wherein nanoelectronics are merged with biological systems in three dimensions. As in any nascent area, opportunities and challenges abound. For example, one could broaden the sensing capabilities to address various disease states, both in vitro (organ on a chip) or in vivo (125), by exploiting the diverse NW building blocks available from chemical synthesis. Cell or tissue interactions with nanoES could be manipulated through modification with cell growth determinants (121). The nanoES could be enhanced to provide electrical and mechanical stimulation to optimize cell culture; in vivo, these properties could provide functionalities such as pacing and moduli that match those of host tissues.

The long-term in vivo biocompatibility of nanoES should be studied. One can envision nanoES-based tissues that are hardwired to provide closed-loop systems that sense and treat disease, enable telemetric monitoring of physiological processes, or connect electronics with the host nervous system.

6. WHAT'S NEXT?

The challenges associated with nanotechnology applications in biomedical sciences are numerous, but their impact on our understanding of how the cardiac and nervous systems work, how they fail in disease, and how we can intervene at a nanoscopic or even molecular level is significant. For example, neural developmental factors, such as the cadherins, laminins, and bone morphometric protein families, as well as their receptors, could be manipulated in new ways (126). Bottom-up NW nanotechnology allows us to explore the functional specificity of these molecules by incorporating them into predefined locations in NW devices to exert highly targeted effects on single cells.

Incorporating nanoelectronics or nanoscience in general into synthetic biology and/or systems biology (46, 47) could be highly rewarding. Doing so would represent a great leap forward in materials sciences and biological sciences, especially because of the many nanoelectronic and nanophotonic devices that one can envision building into cellular circuitry and merging with biological information processing systems, and because we have already achieved intracellular interrogation (31) and 3D electrical innervation of tissues (66) with semiconductor nanoelectronics!

DISCLOSURE STATEMENT

The authors are not aware of any affiliations, memberships, funding, or financial holdings that might be perceived as affecting the objectivity of this review.

ACKNOWLEDGMENTS

B.T. acknowledges support from the University of Chicago and the National Science Foundation Materials Research Centers and Teams. C.M.L. acknowledges support from a National Institutes of Health Director's Pioneer award and a McKnight Foundation Technological Innovations in Neurosciences award.

LITERATURE CITED

1. Comm. Technol., Subcomm. Nano. Sci., Eng., Technol. 2010. *National Nanotechnology Initiative Signature Initiative: Nanoelectronics for 2020 and Beyond.* Washington, DC: US Natl. Nanotechnol. Inst. **http://nano.gov/sites/default/files/pub_resource/nni_siginit_nanoelectronics_jul_2010.pdf**.
2. Ieong M, Doris B, Kedzierski J, Rim K, Yang M. 2004. Silicon device scaling to the sub-10-nm regime. *Science* 306:2057–60
3. Lieber CM. 2011. Semiconductor nanowires: a platform for nanoscience and nanotechnology. *Mater. Res. Soc. Bull.* 36:1052–63
4. Lu W, Lieber CM. 2006. Semiconductor nanowires. *J. Phys. D* 39:387–406R
5. Lu W, Lieber CM. 2007. Nanoelectronics from the bottom up. *Nat. Mater.* 6:841–50
6. Lu W, Xie P, Lieber CM. 2008. Nanowire transistor performance limits and applications. *IEEE Trans. Electron Devices* 55:2859–76
7. Cui Y, Lieber CM. 2001. Functional nanoscale electronic devices assembled using silicon nanowire building blocks. *Science* 291:851–53
8. Duan XF, Huang Y, Cui Y, Wang JF, Lieber CM. 2001. Indium phosphide nanowires as building blocks for nanoscale electronic and optoelectronic devices. *Nature* 409:66–69
9. Friedman RS, McAlpine MC, Ricketts DS, Ham D, Lieber CM. 2005. High-speed integrated nanowire circuits. *Nature* 434:1085
10. Rogers JA, Lagally MG, Nuzzo RG. 2011. Synthesis, assembly and applications of semiconductor nanomembranes. *Nature* 477:45–53
11. Sun Y, Rogers JA. 2007. Inorganic semiconductors for flexible electronics. *Adv. Mater.* 19:1897–916
12. Yan H, Choe HS, Nam SW, Hu YJ, Das S, et al. 2011. Programmable nanowire circuits for nanoprocessors. *Nature* 470:240–44
13. Choi CL, Alivisatos AP. 2010. From artificial atoms to nanocrystal molecules: preparation and properties of more complex nanostructures. *Annu. Rev. Phys. Chem.* 61:369–89
14. Yin Y, Alivisatos AP. 2005. Colloidal nanocrystal synthesis and the organic-inorganic interface. *Nature* 437:664–70
15. Law M, Goldberger J, Yang PD. 2004. Semiconductor nanowires and nanotubes. *Annu. Rev. Mater. Res.* 34:83–122
16. Li Y, Qian F, Xiang J, Lieber CM. 2006. Nanowire electronic and optoelectronic devices. *Mater. Today* 9:18–27
17. Bonaccorso F, Sun Z, Hasan T, Ferrari AC. 2010. Graphene photonics and optoelectronics. *Nat. Photonics* 4:611–22
18. Geim AK. 2009. Graphene: status and prospects. *Science* 324:1530–34
19. Kim K, Choi JY, Kim T, Cho SH, Chung HJ. 2011. A role for graphene in silicon-based semiconductor devices. *Nature* 479:338–44
20. Schwierz F. 2010. Graphene transistors. *Nat. Nanotechnol.* 5:487–96
21. Bjork MT, Ohlsson BJ, Sass T, Persson AI, Thelander C, et al. 2002. One-dimensional heterostructures in semiconductor nanowhiskers. *Appl. Phys. Lett.* 80:1058–60
22. Gudiksen MS, Lauhon LJ, Wang J, Smith DC, Lieber CM. 2002. Growth of nanowire superlattice structures for nanoscale photonics and electronics. *Nature* 415:617–20
23. Yang C, Zhong ZH, Lieber CM. 2005. Encoding electronic properties by synthesis of axial modulation–doped silicon nanowires. *Science* 310:1304–7
24. Jiang XC, Tian BZ, Xiang J, Qian F, Zheng GF, et al. 2011. Rational growth of branched nanowire heterostructures with synthetically encoded properties and function. *Proc. Natl. Acad. Sci. USA* 108:12212–16
25. Lauhon LJ, Gudiksen MS, Wang CL, Lieber CM. 2002. Epitaxial core-shell and core-multishell nanowire heterostructures. *Nature* 420:57–61
26. Dick KA, Deppert K, Larsson MW, Martensson T, Seifert W, et al. 2004. Synthesis of branched "nanotrees" by controlled seeding of multiple branching events. *Nat. Mater.* 3:380–84
27. Algra RE, Verheijen MA, Borgstrom MT, Feiner LF, Immink G, et al. 2008. Twinning superlattices in indium phosphide nanowires. *Nature* 456:369–72

28. Caroff P, Dick KA, Johansson J, Messing ME, Deppert K, Samuelson L. 2009. Controlled polytypic and twin-plane superlattices in III-V nanowires. *Nat. Nanotechnol.* 4:50–55
29. Tian BZ, Zheng XL, Kempa TJ, Fang Y, Yu NF, et al. 2007. Coaxial silicon nanowires as solar cells and nanoelectronic power sources. *Nature* 449:885–88
30. Schwarz KW, Tersoff J, Kodambaka S, Chou YC, Ross FM. 2011. Geometrical frustration in nanowire growth. *Phys. Rev. Lett.* 107:265502
31. Tian BZ, Cohen-Karni T, Qing Q, Duan XJ, Xie P, Lieber CM. 2010. Three-dimensional, flexible nanoscale field-effect transistors as localized bioprobes. *Science* 329:830–34
32. Tian BZ, Xie P, Kempa TJ, Bell DC, Lieber CM. 2009. Single-crystalline kinked semiconductor nanowire superstructures. *Nat. Nanotechnol.* 4:824–29
33. Cohen-Karni T, Timko BP, Weiss LE, Lieber CM. 2009. Flexible electrical recording from cells using nanowire transistor arrays. *Proc. Natl. Acad. Sci. USA* 106:7309–13
34. Fan Z, Ho JC, Jacobson ZA, Razavi H, Javey A. 2008. Large-scale, heterogeneous integration of nanowire arrays for image sensor circuitry. *Proc. Natl. Acad. Sci. USA* 105:11066–70
35. Fan Z, Ho JC, Takahashi T, Yerushalmi R, Takei K, et al. 2009. Toward the development of printable nanowire electronics and sensors. *Adv. Mater.* 21:3730–43
36. Goldberger J, Hochbaum AI, Fan R, Yang P. 2006. Silicon vertically integrated nanowire field effect transistors. *Nano Lett.* 6:973–77
37. Javey A, Nam S, Friedman RS, Yan H, Lieber CM. 2007. Layer-by-layer assembly of nanowires for three-dimensional, multifunctional electronics. *Nano Lett.* 7:773–77
38. McAlpine MC, Friedman RS, Jin S, Lin KH, Wang WU, Lieber CM. 2003. High-performance nanowire electronics and photonics on glass and plastic substrates. *Nano Lett.* 3:1531–35
39. McAlpine MC, Friedman RS, Lieber CM. 2005. High-performance nanowire electronics and photonics and nanoscale patterning on flexible plastic substrates. *Proc. IEEE* 93:1357–63
40. Nam S, Jiang XC, Xiong QH, Ham D, Lieber CM. 2009. Vertically integrated, three-dimensional nanowire complementary metal-oxide-semiconductor circuits. *Proc. Natl. Acad. Sci. USA* 106:21035–38
41. Qing Q, Pal SK, Tian B, Duan X, Timko BP, et al. 2010. Nanowire transistor arrays for mapping neural circuits in acute brain slices. *Proc. Natl. Acad. Sci. USA* 107:1882–87
42. Timko BP, Cohen-Karni T, Yu GH, Qing Q, Tian BZ, Lieber CM. 2009. Electrical recording from hearts with flexible nanowire device arrays. *Nano Lett.* 9:914–18
43. Whang D, Jin S, Wu Y, Lieber CM. 2003. Large-scale hierarchical organization of nanowire arrays for integrated nanosystems. *Nano Lett.* 3:1255–59
44. Yu GH, Cao AY, Lieber CM. 2007. Large-area blown bubble films of aligned nanowires and carbon nanotubes. *Nat. Nanotechnol.* 2:372–77
45. Yu GH, Li XL, Lieber CM, Cao AY. 2008. Nanomaterial-incorporated blown bubble films for large-area, aligned nanostructures. *J. Mater. Chem.* 18:728–34
46. Nandagopal N, Elowitz MB. 2011. Synthetic biology: integrated gene circuits. *Science* 333:1244–48
47. Ruder WC, Lu T, Collins JJ. 2011. Synthetic biology moving into the clinic. *Science* 333:1248–52
48. Slusarczyk AL, Lin A, Weiss R. 2012. Foundations for the design and implementation of synthetic genetic circuits. *Nat. Rev. Genet.* 13:406–20
49. Weber W, Fussenegger M. 2012. Emerging biomedical applications of synthetic biology. *Nat. Rev. Genet.* 13:21–35
50. Khalil AS, Collins JJ. 2010. Synthetic biology: Applications come of age. *Nat. Rev. Genet.* 11:367–79
51. Mukherji S, van Oudenaarden A. 2009. Synthetic biology: understanding biological design from synthetic circuits. *Nat. Rev. Genet.* 10:859–71
52. Patolsky F, Timko BP, Zheng G, Lieber CM. 2007. Nanowire-based nanoelectronic devices in the life sciences. *Mater. Res. Soc. Bull.* 32:142–49
53. Timko BP, Cohen-Karni T, Qing Q, Tian BZ, Lieber CM. 2010. Design and implementation of functional nanoelectronic interfaces with biomolecules, cells, and tissue using nanowire device arrays. *IEEE Trans. Nanotechnol.* 9:269–80
54. Fan ZY, Razavi H, Do JW, Moriwaki A, Ergen O, et al. 2009. Three-dimensional nanopillar-array photovoltaics on low-cost and flexible substrates. *Nat. Mater.* 8:648–53

55. Boettcher SW, Spurgeon JM, Putnam MC, Warren EL, Turner-Evans DB, et al. 2010. Energy-conversion properties of vapor-liquid-solid-grown silicon wire–array photocathodes. *Science* 327:185–87
56. Kelzenberg MD, Boettcher SW, Petykiewicz JA, Turner-Evans DB, Putnam MC, et al. 2010. Enhanced absorption and carrier collection in Si wire arrays for photovoltaic applications. *Nat. Mater.* 9:239–44
57. Garnett E, Yang PD. 2010. Light trapping in silicon nanowire solar cells. *Nano Lett.* 10:1082–87
58. Qin Y, Wang XD, Wang ZL. 2008. Microfibre-nanowire hybrid structure for energy scavenging. *Nature* 451:809–15
59. Xu S, Qin Y, Xu C, Wei YG, Yang RS, Wang ZL. 2010. Self-powered nanowire devices. *Nat. Nanotechnol.* 5:366–73
60. Wang XD, Song JH, Liu J, Wang ZL. 2007. Direct-current nanogenerator driven by ultrasonic waves. *Science* 316:102–5
61. Wang ZL, Song JH. 2006. Piezoelectric nanogenerators based on zinc oxide nanowire arrays. *Science* 312:242–46
62. Kim W, Ng JK, Kunitake ME, Conklin BR, Yang PD. 2007. Interfacing silicon nanowires with mammalian cells. *J. Am. Chem. Soc.* 129:7228–29
63. Chevrier N, Mertins P, Artyomov MN, Shalek AK, Iannacone M, et al. 2011. Systematic discovery of TLR signaling components delineates viral-sensing circuits. *Cell* 147:853–67
64. Shalek AK, Robinson JT, Karp ES, Lee JS, Ahn DR, et al. 2010. Vertical silicon nanowires as a universal platform for delivering biomolecules into living cells. *Proc. Natl. Acad. Sci. USA* 107:1870–75
65. Xie C, Hanson L, Cui Y, Cui BX. 2011. Vertical nanopillars for highly localized fluorescence imaging. *Proc. Natl. Acad. Sci. USA* 108:3894–99
66. Tian BZ, Liu J, Dvir T, Jin LH, Tsui JH, et al. 2012. Macroporous nanowire nanoelectronic scaffolds for synthetic tissues. *Nat. Mater.* 11:986–94
67. Duan XJ, Gao RX, Xie P, Cohen-Karni T, Qing Q, et al. 2012. Intracellular recordings of action potentials by an extracellular nanoscale field-effect transistor. *Nat. Nanotechnol.* 7:174–79
68. Gao RX, Strehle S, Tian BZ, Cohen-Karni T, Xie P, et al. 2012. Outside looking in: nanotube transistor intracellular sensors. *Nano Lett.* 12:3329–33
69. Jiang Z, Qing Q, Xie P, Gao RX, Lieber CM. 2012. Kinked *p-n* junction nanowire probes for high spatial resolution sensing and intracellular recording. *Nano Lett.* 12:1711–16
70. Sakmann B, Neher E. 1984. Patch clamp techniques for studying ionic channels in excitable membranes. *Annu. Rev. Physiol.* 46:455–72
71. Robinson JT, Jorgolli M, Shalek AK, Yoon MH, Gertner RS, Park H. 2012. Vertical nanowire electrode arrays as a scalable platform for intracellular interfacing to neuronal circuits. *Nat. Nanotechnol.* 7:180–84
72. Ewing AG, Strein TG, Lau YY. 1992. Analytical chemistry in microenvironments—single nerve cells. *Acc. Chem. Res.* 25:440–47
73. Schrlau MG, Dun NJ, Bau HH. 2009. Cell electrophysiology with carbon nanopipettes. *Am. Chem. Soc. Nano* 3:563–68
74. Xie C, Lin ZL, Hanson L, Cui Y, Cui BX. 2012. Intracellular recording of action potentials by nanopillar electroporation. *Nat. Nanotechnol.* 7:185–90
75. Bohn PW. 2009. Nanoscale control and manipulation of molecular transport in chemical analysis. *Annu. Rev. Anal. Chem.* 2:279–96
76. Henstridge MC, Compton RG. 2012. Mass transport to micro- and nanoelectrodes and their arrays: a review. *Chem. Rec.* 12:63–71
77. Walsh DA, Lovelock KRJ, Licence P. 2010. Ultramicroelectrode voltammetry and scanning electrochemical microscopy in room-temperature ionic liquid electrolytes. *Chem. Soc. Rev.* 39:4185–94
78. Yeh JI, Shi HB. 2010. Nanoelectrodes for biological measurements. *Wiley Interdiscip. Rev. Nanomed. Nanobiotechnol.* 2:176–88
79. Sze SM. 1981. *Physics of Semiconductor Devices.* New York: Wiley Intersci. 880 pp. 2nd ed.
80. Buzsaki G, Anastassiou CA, Koch C. 2012. The origin of extracellular fields and currents—EEG, ECoG, LFP and spikes. *Nat. Rev. Neurosci.* 13:407–20
81. Plonsey R, Barr RC. 2000. *Bioelectricity—A Quantitative Approach*. Amsterdam: Kluwer Acad./Plenum. 2nd ed.

82. Givargizov EI. 1975. Fundamental aspects of VLS growth. *J. Crystal Growth* 31:20–30
83. Wagner RS, Ellis WC. 1964. Vapor-liquid-solid mechanism of single crystal growth. *Appl. Phys. Lett.* 4:89
84. Cui Y, Lauhon LJ, Gudiksen MS, Wang JF, Lieber CM. 2001. Diameter-controlled synthesis of single-crystal silicon nanowires. *Appl. Phys. Lett.* 78:2214–16
85. Morales AM, Lieber CM. 1998. A laser ablation method for the synthesis of crystalline semiconductor nanowires. *Science* 279:208–11
86. Duan XF, Lieber CM. 2000. General synthesis of compound semiconductor nanowires. *Adv. Mater.* 12:298–302
87. Duan XF, Lieber CM. 2000. Laser-assisted catalytic growth of single crystal GaN nanowires. *J. Am. Chem. Soc.* 122:188–89
88. Cohen-Karni T, Casanova D, Cahoon JF, Qing Q, Bell DC, Lieber CM. 2012. Synthetically encoded ultrashort-channel nanowire transistors for fast, pointlike cellular signal detection. *Nano Lett.* 12:2639–44
89. Lieber CM. 2002. Nanowire superlattices. *Nano Lett.* 2:81–82
90. Wu YY, Fan R, Yang PD. 2002. Block-by-block growth of single-crystalline Si/SiGe superlattice nanowires. *Nano Lett.* 2:83–86
91. Qian F, Gradecak S, Li Y, Wen CY, Lieber CM. 2005. Core/multishell nanowire heterostructures as multicolor, high-efficiency light-emitting diodes. *Nano Lett.* 5:2287–91
92. Hu YJ, Churchill HOH, Reilly DJ, Xiang J, Lieber CM, Marcus CM. 2007. A Ge/Si heterostructure nanowire–based double quantum dot with integrated charge sensor. *Nat. Nanotechnol.* 2:622–25
93. Hu YJ, Kuemmeth F, Lieber CM, Marcus CM. 2012. Hole spin relaxation in Ge-Si core-shell nanowire qubits. *Nat. Nanotechnol.* 7:47–50
94. Lu W, Xiang J, Timko BP, Wu Y, Lieber CM. 2005. One-dimensional hole gas in germanium/silicon nanowire heterostructures. *Proc. Natl. Acad. Sci. USA* 102:10046–51
95. Xiang J, Lu W, Hu YJ, Wu Y, Yan H, Lieber CM. 2006. Ge/Si nanowire heterostructures as high-performance field-effect transistors. *Nature* 441:489–93
96. Wang D, Qian F, Yang C, Zhong ZH, Lieber CM. 2004. Rational growth of branched and hyperbranched nanowire structures. *Nano Lett.* 4:871–74
97. Zhou X, Moran-Mirabal JM, Craighead HG, McEuen PL. 2007. Supported lipid bilayer/carbon nanotube hybrids. *Nat. Nanotechnol.* 2:185–90
98. Kim D-H, Lu N, Ghaffari R, Kim Y-S, Lee SP, et al. 2011. Materials for multifunctional balloon catheters with capabilities in cardiac electrophysiological mapping and ablation therapy. *Nat. Mater.* 10:316–23
99. Viventi J, Kim D-H, Moss JD, Kim Y-S, Blanco JA, et al. 2010. A conformal, bio-interfaced class of silicon electronics for mapping cardiac electrophysiology. *Sci. Trans. Med.* 2:24ra22
100. Viventi J, Kim D-H, Vigeland L, Frechette ES, Blanco JA, et al. 2011. Flexible, foldable, actively multiplexed, high-density electrode array for mapping brain activity in vivo. *Nat. Neurosci.* 14:1599–605
101. Kim DH, Viventi J, Amsden JJ, Xiao JL, Vigeland L, et al. 2010. Dissolvable films of silk fibroin for ultrathin conformal bio-integrated electronics. *Nat. Mater.* 9:511–17
102. Hu YJ, Xiang J, Liang GC, Yan H, Lieber CM. 2008. Sub-100 nanometer channel length Ge/Si nanowire transistors with potential for 2 THz switching speed. *Nano Lett.* 8:925–30
103. Patolsky F, Timko BP, Yu GH, Fang Y, Greytak AB, et al. 2006. Detection, stimulation, and inhibition of neuronal signals with high-density nanowire transistor arrays. *Science* 313:1100–4
104. Mercanzini A, Colin P, Bensadoun JC, Bertsch A, Renaud P. 2009. In vivo electrical impedance spectroscopy of tissue reaction to microelectrode arrays. *IEEE Trans. Biomed. Eng.* 56:1909–18
105. Patrick E, Orazem ME, Sanchez JC, Nishida T. 2011. Corrosion of tungsten microelectrodes used in neural recording applications. *J. Neurosci. Methods* 198:158–71
106. Chernomordik LV, Kozlov MM. 2008. Mechanics of membrane fusion. *Nat. Struct. Mol. Biol.* 15:675–83
107. Kauer JS, White J. 2001. Imaging and coding in the olfactory system. *Annu. Rev. Neurosci.* 24:963–79
108. Grinvald A, Hildesheim R. 2004. VSDI: a new era in functional imaging of cortical dynamics. *Nat. Rev. Neurosci.* 5:874–85
109. Kralj JM, Douglass AD, Hochbaum DR, Maclaurin D, Cohen AE. 2012. Optical recording of action potentials in mammalian neurons using a microbial rhodopsin. *Nat. Methods* 9:90–95

110. Kralj JM, Hochbaum DR, Douglass AD, Cohen AE. 2011. Electrical spiking in *Escherichia coli* probed with a fluorescent voltage-indicating protein. *Science* 333:345–48
111. Hochberg LR, Bacher D, Jarosiewicz B, Masse NY, Simeral JD, et al. 2012. Reach and grasp by people with tetraplegia using a neurally controlled robotic arm. *Nature* 485:372–75
112. Hochberg LR, Serruya MD, Friehs GM, Mukand JA, Saleh M, et al. 2006. Neuronal ensemble control of prosthetic devices by a human with tetraplegia. *Nature* 442:164–71
113. Serruya MD, Hatsopoulos NG, Paninski L, Fellows MR, Donoghue JP. 2002. Instant neural control of a movement signal. *Nature* 416:141–42
114. Truccolo W, Hochberg LR, Donoghue JP. 2010. Collective dynamics in human and monkey sensorimotor cortex: predicting single neuron spikes. *Nat. Neurosci.* 13:105–111
115. Ferrari M. 2008. Beyond drug delivery. *Nat. Nanotechnol.* 3:131–32
116. Nel AE, Mädler L, Velegol D, Xia T, Hoek EMV, et al. 2009. Understanding biophysicochemical interactions at the nano-bio interface. *Nat. Mater.* 8:543–57
117. Rajendran L, Knolker HJ, Simons K. 2010. Subcellular targeting strategies for drug design and delivery. *Nat. Rev. Drug Discov.* 9:29–42
118. Summers HD, Rees P, Holton MD, Brown MR, Chappell SC, et al. 2011. Statistical analysis of nanoparticle dosing in a dynamic cellular system. *Nat. Nanotechnol.* 6:170–74
119. Wylie RG, Ahsan S, Aizawa Y, Maxwell KL, Morshead CM, Shoichet MS. 2011. Spatially controlled simultaneous patterning of multiple growth factors in three-dimensional hydrogels. *Nat. Mater.* 10:799–806
120. Kloxin AM, Kasko AM, Salinas CN, Anseth KS. 2009. Photodegradable hydrogels for dynamic tuning of physical and chemical properties. *Science* 324:59–63
121. Dvir T, Timko BP, Kohane DS, Langer R. 2011. Nanotechnological strategies for engineering complex tissues. *Nat. Nanotechnol.* 6:13–22
122. Hutmacher DW. 2010. Biomaterials offer cancer research the third dimension. *Nat. Mater.* 9:90–93
123. Prestwich GD. 2008. Evaluating drug efficacy and toxicology in three dimensions: using synthetic extracellular matrices in drug discovery. *Acc. Chem. Res.* 41:139–48
124. Prohaska OJ, Olcaytug F, Pfundner P, Dragaun H. 1986. Thin-film multiple electrode probes—possibilities and limitations. *IEEE Trans. Biomed. Eng.* 33:223–29
125. Huh D, Matthews BD, Mammoto A, Montoya-Zavala M, Hsin HY, Ingber DE. 2010. Reconstituting organ-level lung functions on a chip. *Science* 328:1662–68
126. Silva GA. 2006. Neuroscience nanotechnology: progress, opportunities and challenges. *Nat. Rev. Neurosci.* 7:65–74

Annual Review of
Analytical Chemistry

Volume 6, 2013

Contents

Indexes

Errata

An online log of corrections to *Annual Review of Analytical Chemistry* articles may be found at http://arjournals.annualreviews.org/errata/anchem